

Supporting Information

Plasmon-Trion and Plasmon-Exciton Resonance Energy Transfer from a Single Plasmonic Nanoparticle to Monolayer MoS₂[†]

Mingsong Wang^a, Wei Li^{b,c,e}, Leonardo Scarabelli^{f,g,h}, Bharath Bangalore Rajeeva^e, Mauricio Terrones^{k,l,m,n},
Luis M. Liz-Marzán^{f,i,j}, Deji Akinwande^{b,c,e}, Yuebing Zheng^{*,a,e}

^aDepartment of Mechanical Engineering, ^bMicroelectronics Research Center, ^cDepartment of Electrical and Computer Engineering, and ^eMaterials Science & and Engineering Program and Texas Materials Institute, The University of Texas at Austin Austin, TX 78712, USA. Email: zheng@austin.utexas.edu. (Y. B. Z.)

^fBionanoplasmonics Laboratory CIC biomaGUNE Paseo de Miramón 182, 20014 Donostia- San Sebastián, Spain.

^gDepartment of Chemistry and Biochemistry, and ^hCalifornia NanoSystems Institute, University of California, Los Angeles, California 90095, USA.

ⁱIkerbasque, Basque Foundation for Science, 48013 Bilbao, Spain.

^jBiomedical Research Networking Center in Bioengineering, Biomaterials, and Nanomedicine CIBER-BBN, 20014 Donostia- San Sebastián, Spain.

^kDepartment of Chemistry, ^lDepartment of Physics, ^mDepartment of Materials Science and Engineering, and ⁿThe Pennsylvania State University Center for 2-Dimensional and Layered Materials, The Pennsylvania State University, University Park, PA 16802, USA.

1. Experimental setup for optical scattering and transmission measurements

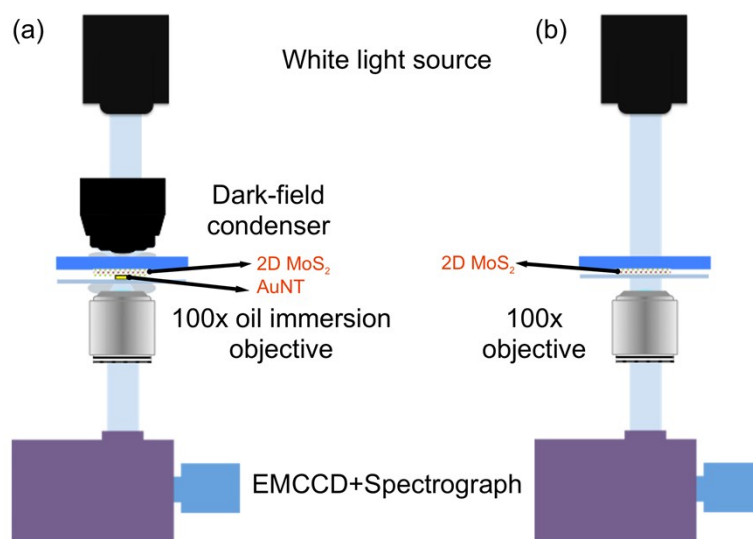


Fig. S1. Schematic of optical setups for (a) dark-field scattering measurement and (b) transmission measurement.

2. Characterization of MoS₂ by atomic force microscopy

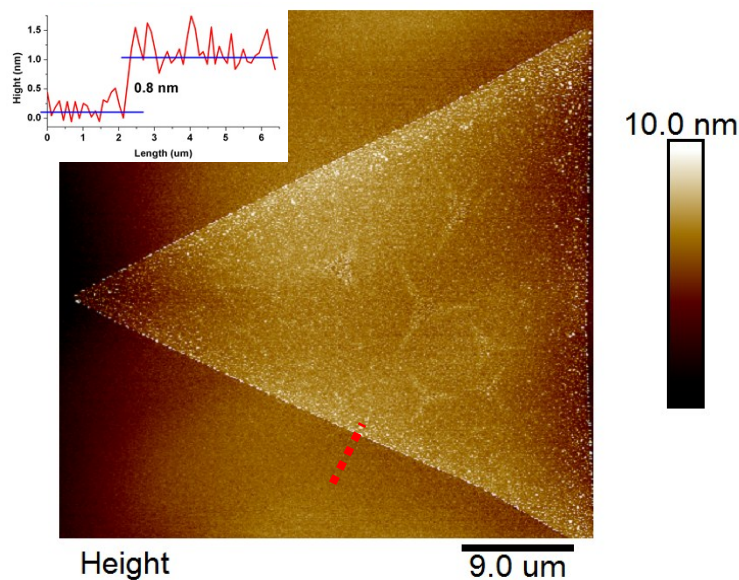


Fig. S2. AFM image of a triangular MoS₂ crystal. Inset is step-height measurement from substrate to monolayer (0.8 nm), as indicated by the red dash line.

Atomic force microscopy (AFM) was applied to measure thickness and morphology of the 2D materials. Fig. S2 shows the AFM image of a typical monolayer crystal with a small bilayer region at its center. The step-height measurement indicates that the CVD-grown MoS₂ film is atomic layer with a thickness of 0.8 nm.

3. Contribution of excitons and trions to the resonance dips in transmission spectra of monolayer MoS₂ and scattering spectra of the AuNT-MoS₂ hybrid

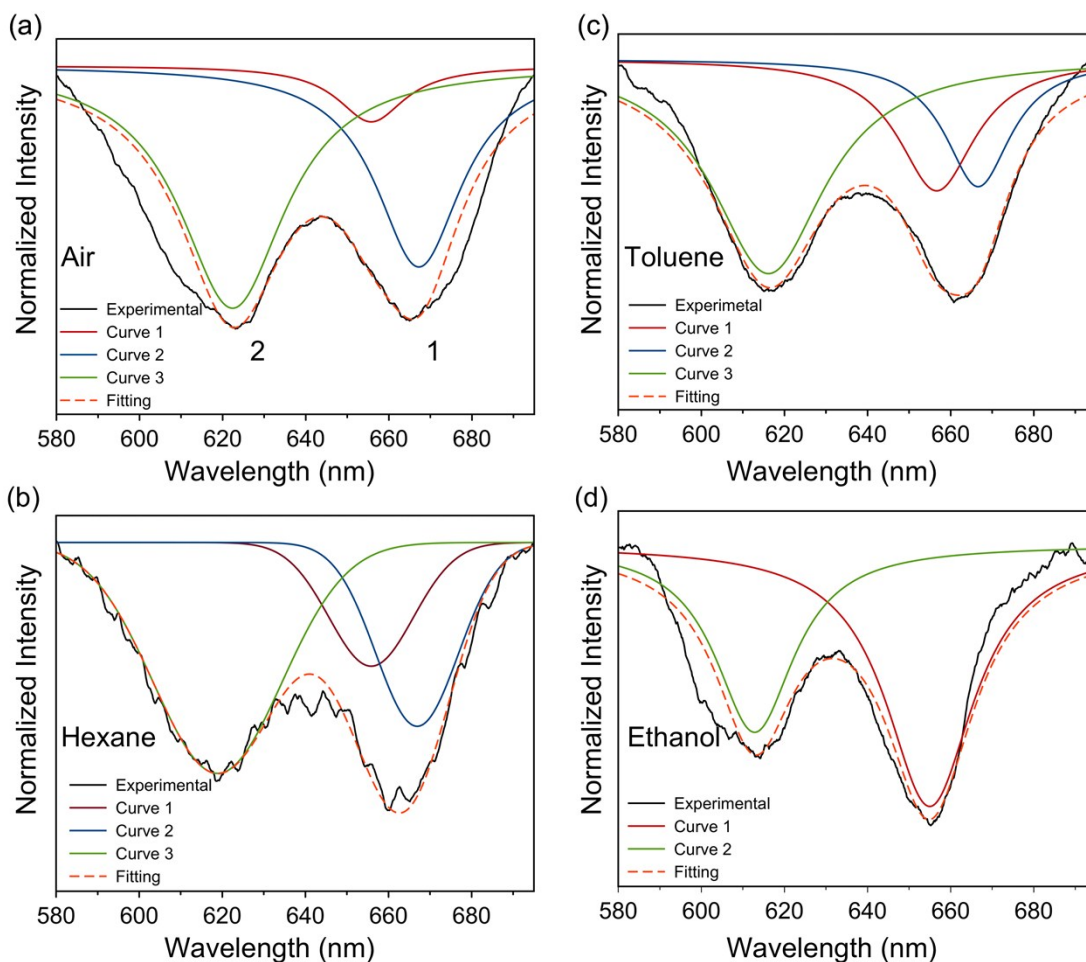


Fig. S3. The fitting curves of the transmission spectra of monolayer MoS₂ in air (a), hexane (b), toluene (c) and ethanol (d). The peaks of the red and blue curve are fixed at 655 nm and 670 nm, respectively.

We fitted the transmission dips in Fig. 2c with Lorentzians. One or two Lorentzians were used to fit the transmission dip 1, and another one was matched with the transmission dip 2. Because the absorption peaks of bare A excitons and bare A⁻ trions are at ~655 nm and ~670 nm at room temperature,¹ we fixed two Lorentzian peaks (the red and blue curve) in Figs. S3a, b and c at these two wavelengths for

fitting the dip 1. Figs. S3a, b and c also show that the depth of A exciton dip (red) increases while that of the A⁻ trion dip (blue) decrease with the dielectric constant of surrounding media. Table S1 summarizes the contribution of excitons and trions to the dip 1. Moreover, as can be seen in Fig. 2c, when monolayer MoS₂ was surrounded by ethanol or water, the dip 1 was at ~655 nm. In this situation, we assumed that there were only excitons in monolayer MoS₂, and the fitted transmission spectrum of monolayer MoS₂ surrounded by ethanol is shown in Fig. S3d as an example. We also found that the contribution of excitons to the transmission dip 1 has a linear relationship with the wavelength of the dip 1, as shown in Fig. S4. Therefore, we assumed the scattering dip 1' in Fig. 6e also follows the same relationship and estimated the contribution of plasmon-exciton and plasmon-trion RET to dip 1' with different surrounding media, as listed in Table S1.

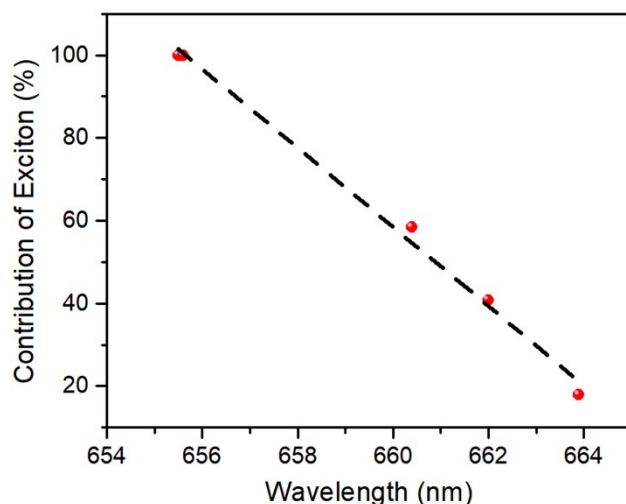


Fig. S4. The linear relationship between the contribution of excitons to dip 1 and the dip 1 wavelength.

Table S1 The estimated contribution of excitons and trions to dip 1 in Fig. 2c and plasmon-exciton and plasmon-trion RET to dip 1' in Fig. 6c.

Surrounding medium	Contribution of exciton (%)	Contribution of trion (%)	Contribution of plasmon-exciton RET (%)	Contribution of plasmon-trion RET (%)
Air	17.9	82.1	20.2	79.8
Hexane	40.8	59.2	58.4	41.6
Toluene	54.8	45.2	77.5	22.5

Ethanol	~100.0	~0	87.0	13.0
Water	~100.0	~0	96.6	3.4

3. TEM images, absorption spectra, and SEM images of AuNTs

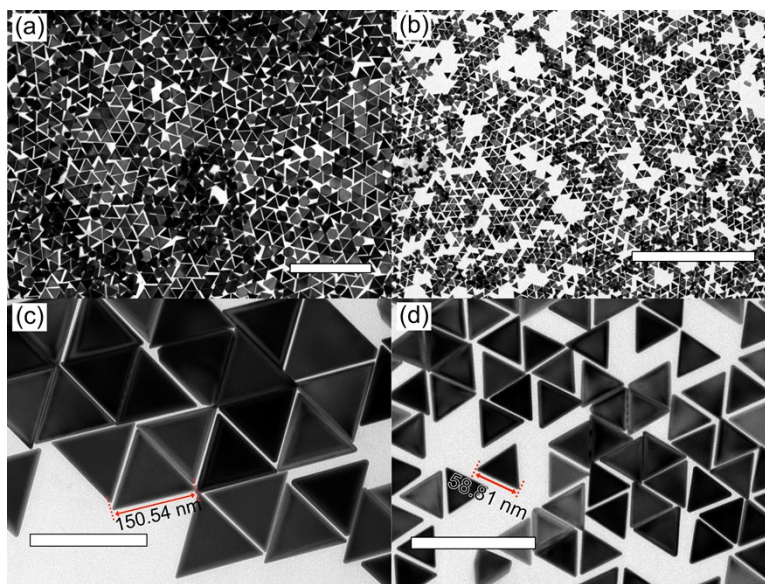


Fig. S5. TEM images of (a) 150 nm and (b) 60 nm Au nanotriangles (AuNTs). Scale bar is 1 μm . High magnification TEM images of (a) 150 nm and (b) 60 nm AuNTs, which show the size of AuNTs. Scale bar is 250 nm.

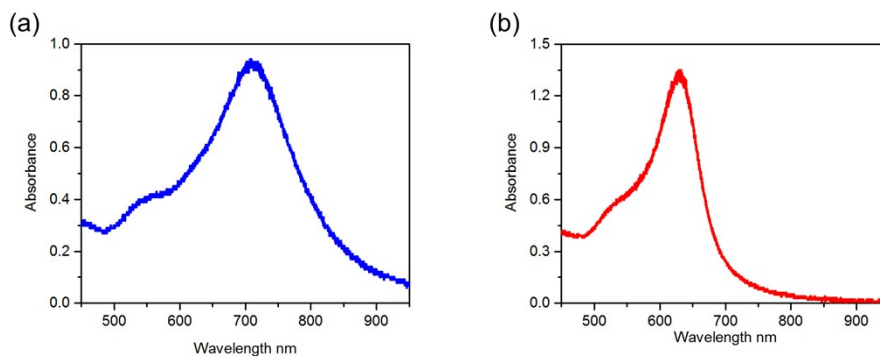


Fig. S6. Absorption spectra of (a) 150 nm and (b) 60 nm AuNTs in solution.

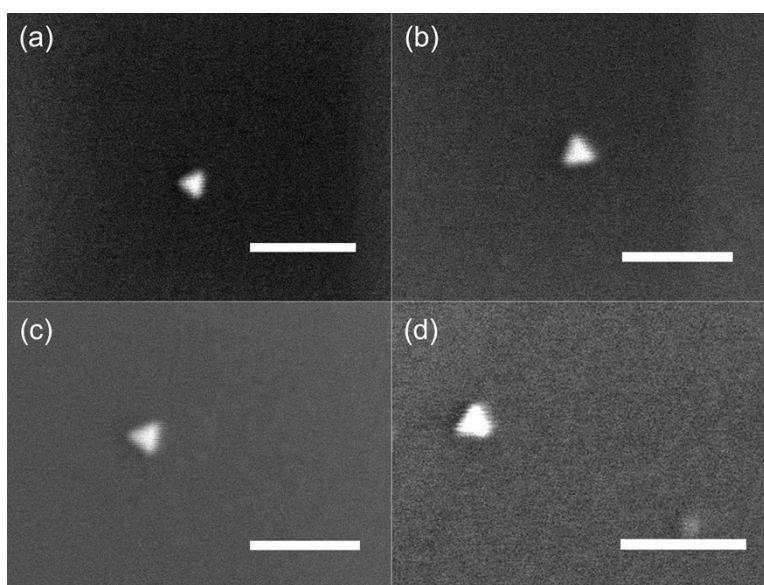


Fig. S7. (a), (b), (c) and (d) SEM images of single AuNTs on monolayer MoS₂.

4. Simulated scattering spectra of a single 150 nm and 60 nm AuNT with different surrounding media.

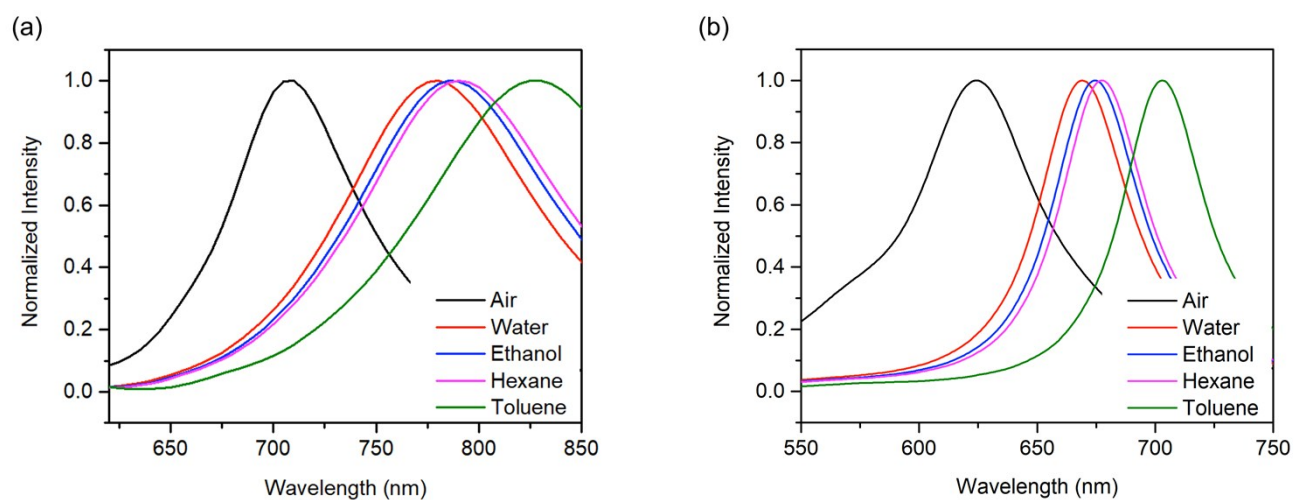


Fig. S8. Simulated scattering spectra of a single 150 nm (a) and 60 nm (b) AuNT.

The FDTD simulation (detailed information is in Experimental part) was used to simulate the scattering spectra of a single 150 nm (a) and 60 nm (b) AuNT, as shown in Fig. S6. The refractive indexes of air (1), water (1.333), ethanol (1.361), hexane (1.375) and toluene (1.497) were used to define those of the

surrounding media. It is worth noticing that the experimental scattering peaks of a single 150 nm AuNT are at slightly shorter wavelengths than the simulated ones. This may be caused by the shape deviation of the synthesized AuNTs to the perfect triangle used in the simulation and the defects in synthesized nanocrystals.

5. Experimental setup for 2D MoS₂ growth

Fig. S9. Schematic of experimental setup for 2D MoS₂ growth from MoO₃ and S precursors.

1. R. Soklaski, Y. Liang and L. Yang, *Appl. Phys. Lett.*, 2014, **104**, 193110.